Regenerative Therapy 18 (2021) 418–429

Contents lists available at ScienceDirect

Regenerative Therapy

journal homepage: http://www.elsevier.com/locate/reth

Original Article

Gelatin hydrogel nonwoven fabrics of a cell culture scaffold to formulate 3-dimensional cell constructs

Toshiki Saotome [a, b], Naoki Shimada [a], Kumiko Matsuno [a, b], Koichiro Nakamura [a, b], Yasuhiko Tabata [b, *]

[a] Research and Development Center, The Japan Wool Textile Co., Ltd, 440, Funamoto, Yoneda-cho, Kakogawa, Hyogo, 675-0053, Japan
[b] Laboratory of Biomaterials, Department of Regeneration Science and Engineering, Institute for Frontier Life and Medical Sciences, Kyoto University, 53 Kawara-cho, Shogoin, Sakyo-ku, Kyoto, 606-8507, Japan

ARTICLE INFO

Article history:
Received 8 August 2021
Received in revised form
9 September 2021
Accepted 29 September 2021

Keywords:
Gelatin hydrogel nonwoven fabrics
3-D culture
Human mesenchymal stromal cells
Hypoxia
ECM remodeling
3-D cell construct

ABSTRACT

The objective of this study is to evaluate the possibility of gelatin hydrogel nonwoven fabrics (GHNF) of a cell culture scaffold to formulate 3-dimensional (3D) cell construct. The thickness of cell construct is about 1 mm and the cells inside are live and bio-active, irrespective of their internal distribution. The GHNF were prepared by the solution blow method of gelatin, following by dehydrothermal crosslinking. The GHNF showed a mechanical strength strong enough not to allow the shape to deform even in a wet state. The wet GHNF also showed resistance against repeated compression. After human mesenchymal stromal cells (hMSC) were seeded and cultured, the inner distribution in GHNF, the apoptosis, hypoxia inducible factor (HIF)-1α, Ki67, collagen or sulfated glycosaminoglycan (sGAG) secretion of cells were evaluated. The hMSC proliferated inside the GHNF with time while a homogeneous distribution in the number of cells proliferated from the surface to the 1000 μm depth of GHNF was observed. The number of apoptosis and HIF-1α positive cells was significantly low compared with that of polypropylene nonwoven fabrics with the similar fiber diameters and intra-structure. The GHNF were degraded during cell culture, and completely replaced by collagen and sGAG secreted. It is concluded that the GHNF is a promising cell culture scaffold for 3D cell constructs.

1. Introduction

One of the realistic strategies to enhance and maintain the biological activities of cells is to achieve 3-dimensional (3D) cell–cell interaction in the *in vivo* condition [1]. As trials to formulate 3D cell constructs *in vitro*, several approaches have been investigated [1,2] to demonstrate the advantages of 3D cell constructs over 2D ones, such as the promotion of cell differentiation [3], the improvement of cell functions [4], the enhancement of drug sensitivity [5–7], and an increased survival of cells after implantation [8]. Among them, 3D cell culture scaffolds have been prepared from different materials in various designs for both the *in vitro* and *in vivo* usages. It has been demonstrated that the porous structures of scaffolds can provide cells with spaces for their proliferation, migration, and differentiation or the promoted construction of cell niche [9,10]. However, one of the big problems for 3D constructs is the death and functional loss of cells due to the poor supply of nutrients and oxygen to cells. When the thickness of cell constructs becomes larger than 150–200 μm, nutrients and oxygen do not reach to the construct inside, resulting in cell necrosis inside the construct [11–14]. Hypoxia often makes cells to decrease the functions and die [13,17,19]. To rescue cells from their hypoxia, several experimental trials, such as the promotion of angiogenesis [11,12], the addition of oxygen releasing materials [15,16], the usage of gas permeable cell culture system [17,18], the design of interconnected porous structure [19], and the incorporation of hydrogels [20–24] have been reported. However, these are still some rooms to be improved for this issue.

* Corresponding author. Laboratory of Biomaterials, Department of Regeneration Science and Engineering, Institute for Frontier Life and Medical Sciences, Kyoto University, 53 Kawara-cho, Shogoin, Sakyo-ku, Kyoto, 606-8507, Japan. Fax: +81 75 751 4646.
E-mail address: yasuhiko@infront.kyoto-u.ac.jp (Y. Tabata).
Peer review under responsibility of the Japanese Society for Regenerative Medicine.

https://doi.org/10.1016/j.reth.2021.09.008

Gelatin hydrogel is one of cell friendly materials available for cell culture substrates. Because it has an inherent property of biocompatibility [25,26], and shows a nature to improve cellular hypoxia [22]. The gelatin hydrogel has a high permeability of oxygen and nutrients through the water phase in hydrogels. It is experimentally confirmed that the incorporation of gelatin hydrogels in 3D cell constructs enables cells to enhance their survival rate and biological functions [21–24].

Based on the characteristics, the gelatin hydrogels of a sponge shape have been widely used, but the poor mechanical strength should be considered for the usage of cell culture substrate [27–29]. This property is one reason of difficulty to maintain their porous structure and interconnectivity during the cell culture. Some trials are reported to tackle the mechanical properties issue of gelatin hydrogels [27–29], but these trial used other additional components or chemical reagents. As one of the formulation strategies to overcome the problems, we have designed a nonwoven fabric of gelatin hydrogels [24,30].

This study is undertaken to evaluate that feasibility of gelatin nonwoven fabrics (GHNF) as a 3D cell culture scaffold by comparing with polypropylene [31] nonwoven fabrics (PPNF) with the same property and structure of GHNF. Following the culture of human mesenchymal stromal cells (hMSC) with the GHNF, the cell proliferation or distribution, hypoxia, apoptosis cells, cell proliferating activity, the secretion of collagen and sulfated glycosaminoglycan (sGAG) inside the cell-GHNF construct. We examine the degradation profile of GHNF with time and the consequent structural component change.

2. Materials and methods

2.1. Preparation of GHNF

The gelatin hydrogel nonwoven fabrics (GHNF) were prepared by the solution blow spinning method previously reported [24,30,32]. Briefly, aqueous solution of 37.5 wt% gelatin with an isoelectric point at 5.0, (Nitta Gelatin Inc., Osaka, Japan), was heated at 60 °C. The gelatin solution was discharged through a nozzle with an internal diameter of 250 μm at different discharge pressures (0.1, 0.15, 0.2, and 0.25 MPa). The discharged gelatin solution was blown by a heated air for dry solidification, followed by collection by a collector to obtain GHNF. Then, the GHNF prepared were freeze-dried for 72 h. The dried and non-crosslink GHNF were treated in a vacuum oven at 140 °C and 1×10^{-5} MPa for 48 h to allow their to dehydrothermally crosslink according to the method previous reported [33]. The cross-linked GHNF were punched out into discs of 4 mm in diameter. The GHNF discs were swollen in 1 mM phosphate-buffered solution (PBS) at 37 °C for 15 min. The weight, thickness, disc diameter, and the fiber diameter of swollen GHNF were measured, while the surface area of swollen GHNF was calculated. The total fiber volume, fiber length, fiber surface area of GHNF, and surface area per unit volume were calculated as below.

$$\text{Total fiber volume per scaffolf } \left(\text{mm}^3\right) = \frac{\text{Weight of swollen GHNF (mg)}}{\text{Density of swollen gelatin (mg/ mm}^3)}$$

$$\text{Fiber length per scaffold (mm)} = \frac{\text{Total fiber volume per scaffold(mm}^3)}{\text{Cross section area of swollen gelatin fiber (mm}^2)}$$

$$\text{Fiber surface area per scaffold(mm}^2) = \text{Fiber diameter(mm)} \times \text{Fiber length (mm)} \times \pi$$

$$\text{Surface area per unit volume} = \frac{\text{Fiber surface area per scaffold(mm}^2)}{\text{Scaffold volume(mm}^3)}$$

After the excess water was removed with paper, the weight of GHNF in the swollen state was measured. The density of swollen gelatin was calculated from the weight and volume of swollen gelatin film which are prepared from same gelatin solution concentration and dehydrothermal crosslinking condition of GHNF. As a control, polypropylene fiber nonwoven fabrics (PPNF) were prepared with the same diameter and structure by the needle punch method [34,35]. Both the GHNF and PPNF were placed in each well of 96 multi-wells plate (Corning® 96 well TC-treated Microplates, Corning incorp., USA) and sterilized using ethylene oxide gas.

2.2. Characterization of GHNF

To observed the appearance and intra-structure of GHNF and PPNF in a dried or swollen condition, scanning electron microscope (SEM, FlexSEM 1000, Hitachi High Technologies corp., Japan) and a light microscope (BX-X710, Keyence Corp., Japan) pictures were taken. For the SEM observation, GHNF and PPNF dried were placed on a stage and fixed with a conductive tape, and then coated with sputtered gold by sputter coater (MSP-1S; Vacuum Device Inc., Japan). The diameter of 50 fibers was measured from the SEM and light microscopic pictures, and the average diameter was calculated by the computer software (PhotoRuler, Hyogo, Japan) and Image J.

Mechanical tests were done on Micro Autograph MST-I (Shimadzu Corp., Japan) with 2 flat-surface compressive stages. The GHNF dried or swollen and PPNF dried were placed between the stages and the compressive stress–strain curves were recorded. The top stage was set to move downward at 1 mm/min from 0% strain to 70% strain. The compressive modulus was calculated from the stress–strain curves with strain ranges of 1–5%. To evaluate the recoverability of GHNF swollen, the same compressive stress–strain test was repeated 10 times for the same sample. At time intervals of each test, the stage position was set to the start position, and the same stress at 0% strain was applied. Immediately after that, the next test was started.

2.3. Cell culture

Human bone marrow derived mesenchymal stromal cells (hMSC) immortalized by introducing human telomerase reverse transcriptase were kindly provided by Dr. Toguchida [36]. hMSC were cultured in 100 mm dish with Minimal Essential Medium alpha (MEMα) (Thermo Inc., Waltham, USA) supplemented with 10 vol% fetal bovine serum (FBS) (Thermo Inc., Waltham, USA) and 1 vol% penicillin and streptomycin (Nacalai tesque, Kyoto, Japan) at 37 °C in a humidified incubator with 5% CO_2. The cells were detached with 0.25 wt% trypsin-containing 1 mM EDTA solution (Nacalai Tesque. Inc., Kyoto, Japan), and continued to culture in 100 mm cell culture dish (Corning Inc., Corning, NY) to allow them to grow until to 80% confluency.

2.4. Cell seeding and culture in GHNF

Before the cell seeding, 200 μl of PBS was dropped onto the dried GHNF and PPNF and left at room temperature for 30 min.

After PBS was removed by pipetting, hMSC (18–19 passaged) cell suspension (200 μl) was seeded onto the GHNF and PPNF at 1×10^6 cells/ml. Next, the hMSC-seeded GHNF and PPNF were agitated on an orbital shaker (Optima Inc., Japan) at 300 rpm for 4 h. The shaking culture is one methodology to make cells homogeneously distribute in the 3D scaffold [37].

The cell-GHNF and cell-PPNF constructs were immobilized with 22G spinal needles (TOP Corp., Japan). The GHNF and PPNF immobilized were set in a spinner flask (Adjustable Hanging Bar Flat Bottom Spinner Flask 250 ml, Bellco Corp., NJ, USA) by stung needles top of flask. The schematic illustration of this cell culture procedure is shown Fig. 2A. The cell manipulation was performed in a clean bench at room temperature for 3 h. The spinner flask placed onto magnetic stirrer (4 position stirrer, Wakenyaku Co. Ltd., Kyoto, Japan) and stirred at 60 rpm for the initial 1 day and at 70 rpm for the following 34 days. The half volume of medium was exchange every 3 or 4 days. The cell-GHNF constructs were cultured for 1 day after the stirred culture, and then cultured for 4, 7, 14, 25, and 35 days by stirring culture.

2.5. Cell proliferation assay

The number of cells proliferated in GHNF and PPNF was evaluated by the DNA assay [38,39]. Briefly, the cell-GHNF and PPNF constructs cultured were washed with the PBS solution three times, and stored at −30 °C until to the assay. After thawing, cells in the GHNF and PPNF were lysed by 30 mM saline-sodium citrate (SSC) containing 0.2 mg/ml sodium dodecyl sulfate (Nakalai Tesque Inc., Japan) at 37 °C, 300 rpm for 24 h by thermomixer (Eppendorf Co. Ltd., Germany). The dye solution of 30 mM SSC containing 1.25 μl/ml Hoechst 33,258 DMSO solution (1 mg/ml, Nakalai tesque, Japan) (160 μl) and the cell lysate (40 μl) was mixed in each well of 96 multi well black flat bottom plate (Corning Inc., NY), while the fluorescence intensity of mixed solution was measured at excitation and emission wavelengths of 355 and 460 nm on fluorescence spectrometer (SpectraMax; Molecular Devices, California, USA). The number of cells was calculated by a standard curve between the fluorescent intensity and cell number known. The DNA assay was performed for 4 materials at each time point and the average number of cells was calculated.

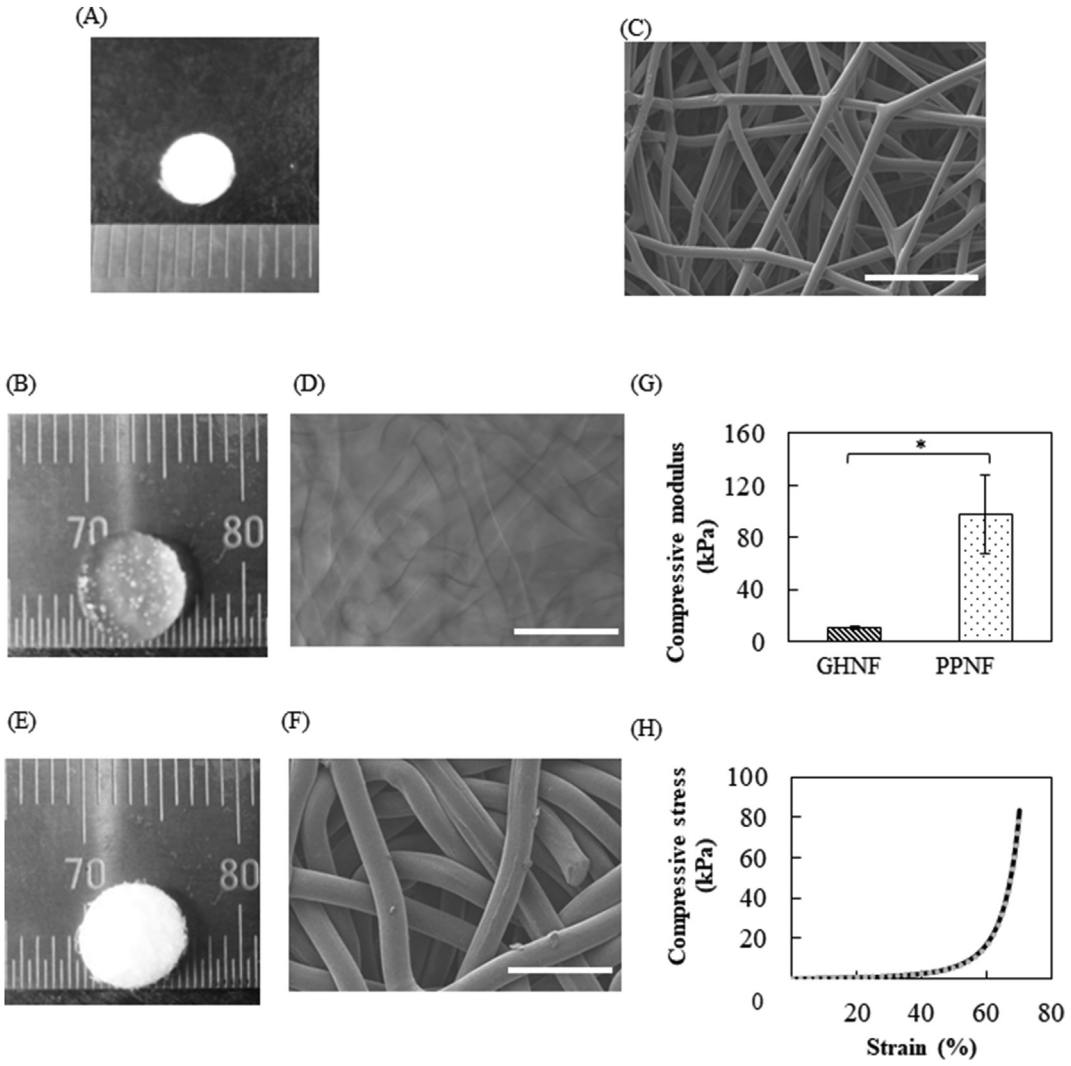

Fig. 1. Light microscope and SEM pictures and mechanical properties of GHNF and PPNF. Light microscopic pictures of GHNF in the dried (A) or swollen state (B). SEM and light microscopic pictures of GHNF in the dried (C) or swollen (D). Light microscope (E) and SEM pictures (F) of PPNF. (G) Compressive Modulus of GHNF and PPNF. (H) Stress– strain curves of GHNF in the swollen state; (–) one time and (- -) 10 times repeated compression stress. The scale bar indicates 200 μm *, $p < 0.05$; significant difference between the groups.

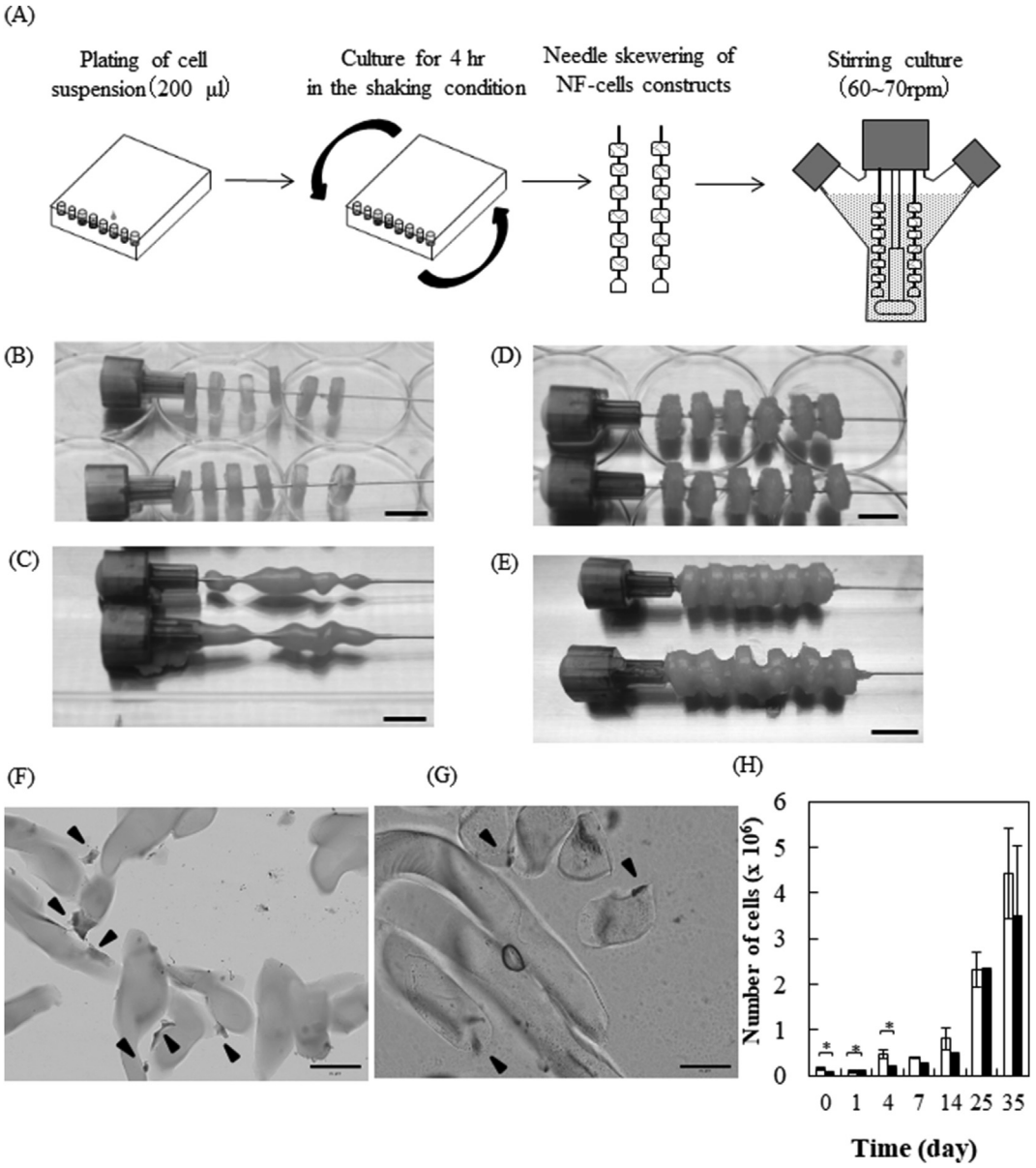

Fig. 2. 3D stirring culture of hMSC in GHNF or PPNF. (A) Schematic illustration of cell culture procedures. Appearance of GHNF (B, C) and PPNF (D, E) before stirring culture (B, D) or 35 days after culture (C, E). HE staining images of GHNF (F) and PPNF (G) cross-sections before stirring culture. The black arrowhead indicates the cell nucleus. (H) Time course of cells proliferation for GHNF (□) and PPNF (■). The scale bar indicates 5 mm (B, C, D, E) and 50 μm (F, G). *, $p < 0.05$; significant difference between the groups.

2.6. Histological examinations

The cell-GHNF or -PPNF constructs were fixed with 4 wt% paraformaldehyde/PBS solution for 15 min, and then washed by PBS 3 times. The samples were placed into 30 wt% sucrose/PBS solution overnight, followed by the embedment in the OCT compound (Sakura Finetek Japan Co. Ltd., Tokyo, Japan) and frozen by liquid nitrogen. The frozen samples were sliced at 10 μm thickness by a cryotome (CM3050S, Leica Microsystems, Wetzlar, Germany) and the resulting sections were transferred to adhesion microscope slides (Matsunami Ind. Ltd., Osaka, Japan) with an adhesive film [40] (Cryofilm type 2C (10); Section Lab Co. Ltd., Japan).

For the hematoxylin and eosin (HE) staining of cross-sectionally sliced section, first the coverage by water-soluble embedment (Aquatex; Merck Ltd., Darmstadt, Germany) to inhibit the fiber shrinkage in the swollen GHNF condition [30], and then stained according to the conventional procedure. The stained sections were observed immediately by light microscope (BX-X710, Keyence Corp., Japan) within one day after embedment. The same procedure of sections preparation was performed for other stained samples unless mentioned especially. The TUNEL staining was performed using In Situ Cell Death Detection Kit, POD (Roche, Germany) according to the user instruction. Apoptotic cells were detected by DAB chromogen (DAKO, CA, USA) for approximately 1 min while the samples counter-stained with hematoxylin. To detect hypoxia and proliferating cells, HIF-1α and Ki67 immunostaining were performed. Briefly, the sections were washed with PBS for 15 min at room temperature, and then the permeabilized 3 times with PBS containing 0.1 wt% Triton X-100 for 5 min at room temperature. Next, the sections were incubated 3 vol% hydrogen peroxide in methanol for 10 min to block the endogenous peroxidase activity and washed PBS for 5 min 2 times. The samples were treated overnight at 4 °C with HIF-1α mouse monoclonal (ESEE122) antibody (1:100 dilution; 14-9100-82; eBioscience Inc., San Diego, USA)

or Ki67 rabbit monoclonal (SP6) antibody (1:5000; ab16667; Abcam plc, Cambrige, UK) in 1x tris-buffered saline solution (TBS) containing 1 wt% bovine serum albumin (Nakalai Tesque, Kyoto, Japan). After washed with TBS containing 0.1% Triton X-100 for 5 min at 2 times, the sections were incubated polymer conjugated 2nd antibody (Histofine Simple Stain MAX PO; Nichirei Bioscience Inc., Japan) for 30 min. After PBS washing, HIF-1α and Ki67 positive cells were detected by the DAB chromogen substrate and counter-stained with hematoxylin. To evaluate cell distribution in GHNF, cells were observed at different depth ranges of GHNF and PPNF, 0–200, 200–400, 400–600, 600–800, and 800–1000 μm depth from the surface. The sections were prepared from 3 different scaffolds at each time point, and cells were counted from each divided images unless mentioned otherwise. The distribution of TUNEL-positive cells and HIF-1α-positive cells were calculated as the number percentage of positive cells to the total cells. The number of Ki67-positive and -negative cells were also counted at different depth ranges from the scaffold surface.

2.7. Secretion assay of collagen and sGAG

As one measure of cell functions, the secretion and distribution of collagen and sulfated glycosaminoglycan (sGAG) in GHNF and PPNF were measured. The sirius red/fast green staining was performed to stain collagen-positive area in the scaffold [41]. The sections were washed by PBS for 20 min and incubated in the sirius red/fast green dye solution (Sirius Red/Fast Green Collagen Staining kit; Chondrex Inc., WA, USA) for 3 min. Then, the sections were washed by double-distilled water (DDW) until the water color becomes clear, followed by immediately observed by the light microscope. Collagen was colored in dark purple while gelatin and cytoplasm were in pink and green, respectively. The alcian blue (pH 1.0) staining was performed to stain sGAG-positive area in the scaffold [42]. The sections were washed by PBS for 20 min and 0.1 N HCl aqueous solution (Muto Pure Chemicals Co. Ltd., Tokyo, Japan) for 1 min, and then incubated in alcian blue (pH 1.0) dye solution (Muto Pure Chemicals Co. Ltd., Tokyo, Japan) for 60 min at room temperature. Next, the sections were incubated in 0.1 N HCl aqueous solution for 3 min and washed by DDW, and then, counter-stained with hematoxylin. sGAG was colored in light blue while gelatin and cell were light purple and dark blue.

To evaluate the distribution of collagen and sGAG secreted, their area was calculated at different depth ranges. The area of collagen and sGAG was analyzed by image J software. Briefly, the images of sirius red/fast green and alcian blue staining were binarized to collagen- or sGAG-positive area respectively. The image binarization were utilized for separate the collagen- or sGAG-positive area from gelatin fiber area which is slightly stained by the sirius red and alcian blue staining.

2.8. Statistical analysis

Results were expressed as the means ± SD of 3 different samples. Statistical significance of differences between the two mean values was performed by the student t-test. The p-value < 0.05 was to be considered statistically significant.

3. Results

3.1. Characterization of GHNF

Fig. 1 shows the pictures and mechanical properties of GHNF and PPNF. Table 1 summarizes the characteristic of GHNF and PPNF. The GHNF had the similar properties and structure to the PPNF. GHNF had a network structure with gelatin fibers melt-jointed at the cross-point (Fig. 1C).

The diameter of gelatin fibers was easily controlled by changing the discharged pressure of gelatin solution in fiber preparation with ranges from 42.6 ± 1.96 to 59.4 ± 5.77 μm (Supporting Figures 1A, 1C, and 1E). As the fiber diameter of GHNF became thicker, the stress–strain curves at the 1st time and the 10th times were not overlapped at a large strain. The findings indicate that GHNF consisting of smaller diameter fibers (42.6 ± 1.96 μm) was good in terms of the compressive recovery property (Supporting Figure 1B). In this study, the fiber diameter of GHNF was selected at 42.6 ± 1.96 μm. The GHNF swollen was transparent while the fiber diameter became larger than that in dried state. The compressive modulus of PPNF was significantly large compared with that of GHNF (Fig. 1G). For the cyclic compressive recovery property, there was no difference in the compressive stress–strain curves of GHNF between one time and 10 times repeated testing (Fig. 1H).

3.2. Cell proliferation in GHNF and PPNF

The 3D cell culture by the stirring method was performed for GHNF and PPNF. Fig. 2A illustrates the experimental procedure. Fig. 2 shows the appearance and inner images for GHNF and PPNF at different time points. The original GHNF was of a disk shape (Fig. 2B), but after 35 days culture, they became smaller (Fig. 2C). Cells proliferate inside GHNF while the GHNF were degraded to form the cell aggregates (called as, the GHNF-based cell aggregates). With incubation, the cell aggregates fused to each other to form a large aggregates (Fig. 2C). On the other hand, the PPNF became thicker with culture time (Fig. 2D and E). Cells were attached onto the fibers surface for both of GNNF and PPNF (Fig. 2F and G). The number of cells proliferated in a GHNF were significantly larger than that of PPNF 0, 4 and 7 days after culture (Fig. 2H).

3.3. Distribution of HE, TUNEL, HIF-1 α, and Ki67-positive cells in GHNF and PPNF

Fig. 3 shows the distribution of HE-positive cells in the GHNF and PPNF at different culture days and the scaffold degradation behavior. With the culture time, the profile of cells infiltrated into the GHNF and PPNF changed. Cells were infiltrated and proliferated in both of GHNF and PPNF after 7 days culture. After 14 and 25 days cultures for the GHNF, many cells were infiltrated into NF while the surface covering of cells with a thin layer was observed (Fig. 3E-H). After 35 days culture, cells aggregates were seen at 500–800 μm depth from the surface (Fig. 3I and J). On the contrary, although cells infiltration into the PPNF was observed, a thick layer was covered on the surface (Fig. 3O-T). The gelatin fibers in the GHNF were degraded with the culture time and the shape changed whereas the shape of PP fibers did not change. The cross-section of gelatin fibers was spherical for the surface and center of GHNF at after cell seeding and 7 days culture after (Fig. 3-D). The gelatin fibers were degraded to adhere together around the surface of GHNF 14 days after culture (Fig. 3E). On 25 days, the gelatin fibers adhered became thinner, but the GHNF maintained a porous structure (Fig. 3G). On the other hand, the shape of gelatin fibers did not change at the center of GHNF (Fig. 3F and H). On 35 days culture, most of gelatin fibers disappeared both on the surface and in the center of GHNF (Fig. 3I and J).

Fig. 4A and B shows the number of HE-positive cells after culture for 14 and 35 days. On 35 days culture, the gelatin fibers of GHNF disappeared and a large aggregate was formed by binding 2 neighboring cell-GHNF constructs (Fig. 4C). The number of cells proliferated in GHNF tended to became small with an increase in the depth from the scaffold surface. However, many cells were present in the

Table 1
Material properties of GHNF and PPNF in the swollen state.

Type	Nonwoven fabrics diameter (mm)	Nonwoven fabrics thickness (mm)	Nonwoven fabrics volume (mm^3)	Nonwoven fabrics weight (mg)	Fiber diameter (μm)	Surface area of fiber (mm^2)	Surface area of fiber per nonwoven fabrics volume (mm^2/mm^3)
GHNF	6.01 ± 0.15[a)]	1.65 ± 0.11	46.9 ± 4.89	22.4 ± 2.67	45.2 ± 5.50	2001 ± 238	42.6 ± 1.96
PPNF	6.00 ± 0.00	1.56 ± 0.05	44.1 ± 1.46	21.0 ± 1.19	52.5 ± 3.93	1754 ± 1.15	39.8 ± 1.51

[a] Mean ± SD.

GHNF even at 600–1000 μm depth range 14 and 35 days later. On the contrary, few cells were observed in the PPNF at the same depth range (Fig. 4A and B). Fig. 4G and H shows the percentage of TUNEL-positive cells 14 and 35days after culture. The percentage of TUNEL-positive cells became large as the depth became deeper. On 14 days culture, the percentage of TUNEL-positive cells for the GHNF at 600–1000 μm depth was less than 50%, whereas that of PPNF was over 80% (Fig. 4G). On 35 days culture, the percentage of TUNEL-positive cells at 400–800 μm depth of GHNF was significantly smaller than that of PPNF (Fig. 4H). The number of TUNEL-negative cells of GHNF at 400–800 μm depth was significantly larger than that of PPNF, although some cells were TUNEL-positive (Fig. 4I-L). Fig. 4M and N show the percentage of HIF-1α-positive cells 14 and 35 days after culture. The percentage of HIF-1α-positive cells became large with an increase in the depth of scaffold. On 14 days culture, the percentage of HIF-1α-positive cells at 400–1000 μm depth for the GHNF was less than 40%, whereas that of PPNF was over 68% (Fig. 4M). After 35 days culture, the percentage of HIF-1α-positive cells at 400–600 μm depth of GHNF was significantly smaller than that of PPNF (Fig. 4N). The number of HIF-1α-negative cells of GHNF at 550–850 μm depth was significantly larger than that of PPNF, although some cells were HIF-1α-positive (Fig. 4O-R).

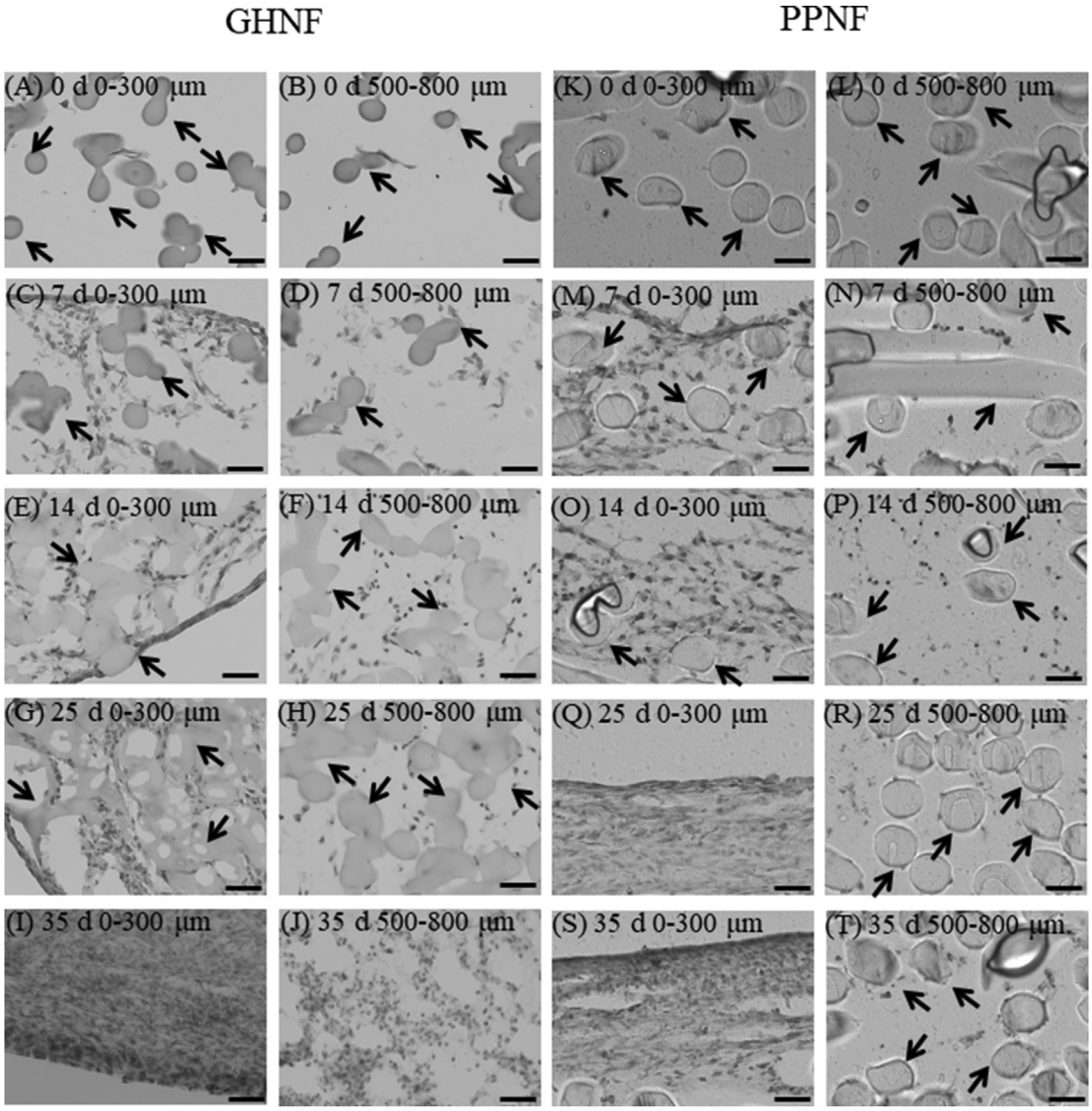

Fig. 3. Time change of HE-positive cells images of GHNF (A, B, C, D, E, F, G, H, I, J) and PPNF(K, L, M, N, O, P, Q, R, S, T) edge (A, C, E, G, I, K, M, O, Q, S) and center (500–800 μm depth) (B, D, F, H, J, L, N, P, R, T). 0 (A, B, K, L), 7 (C, D, M, N), 14 (E, F, M, N), 25 (G, H, Q, R), and 35 days after stirring culture (I, J, S, T). The black arrow indicates the fiber of NF. The scale bar indicates 50 μm.

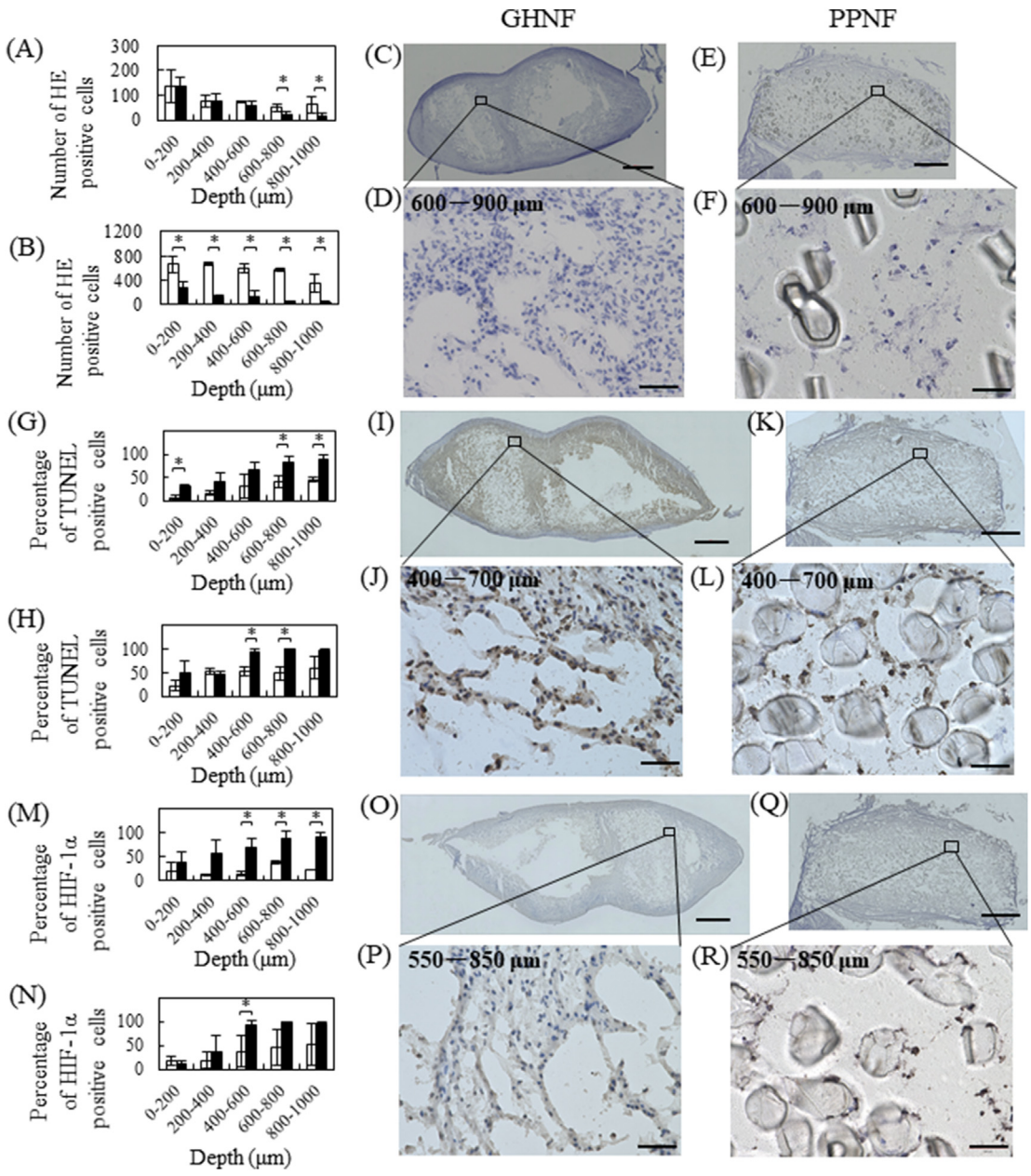

Fig. 4. Distribution of HE-, TUNEL-, and HIF-1α-positive cells in GHNF and PPNF 14 and 35 days after stirring culture. Depth profiles of HE-positive cells in GHNF (□) and PPNF (■) 14 (A) and 35 days (B) after stirring culture. The cross-sectional images of GHNF (C, E) and PPNF (D, F) 35 days after stirring culture. HE images at 600–900 μm depth from the surface of GHNF (D) and PPNF (F). Depth profiles of TUNEL-positive cells in GHNF (□) and PPNF (■)14 (G) and 35 days after stirring culture (H). The cross-sectional images of GHNF (I, J) and PPNF (K, L) 35 days after stirring culture. TUNEL staining images at 400–700 μm depth from the surface of GHNF (J) and PPNF (L). Depth profiles of HIF-1α-positive cells in GHNF (□) and PPNF (■)14 (M) and 35 days after stirring culture (N). The cross-sectional images of GHNF (O, P) and PPNF (Q, R) 35 days after stirring culture. HIF-1α staining images at 550–850 μm depth from the surface of GHNF (P) and PPNF (R). The scale bar indicates 1 mm (C, E, I, K, O, Q) and 50 μm (D, F, J, L, P, R). *, $p < 0.05$; significant difference between the two groups.

Fig. 5A and B shows the number of Ki67-positive and -negative cells 35 days after culture. The number of Ki67-positive cells for the GHNF at 600–1000 μm depth was larger than that of PPNF (Fig. 5A, C-F). Moreover, the same significantly larger number of Ki67-negative cells was seen at 400–1000 μm depth for the GHNF (Fig. 5B–F).

3.4. Distribution of sirius red and alcian blue positive area in GHNF and PPNF

Fig. 6A shows the distribution of sirius red-positive area in GHNF and PPNF. The sirius red stained area tended to decrease with an increased depth for both GHNF and PPNF after 35 days culture. However, the area at 800–1000 μm depth for the GHNF was significantly larger than that of PPNF. Fig. 6B shows the distribution of alcian blue-positive area. The alcian blue stained area tended to decrease with an increased depth for both GHNF and PPNF on 35 days culture. However, the area at 0–1000 μm depth in GHNF was significantly larger than that of PPNF. Fig. 6C–N shows sirius red staining images at different depth ranges of GHNF and PPNF on 35 days culture. The secreted collagen fiber in the GHNF at 200–800 μm depth was thick and bundle-shaped (Fig. 6I, K, and M), whereas that of PPNF was thin and spread-shaped (Fig. 6J, L, and N). Fig. 6O–Z shows alcian blue staining images at different

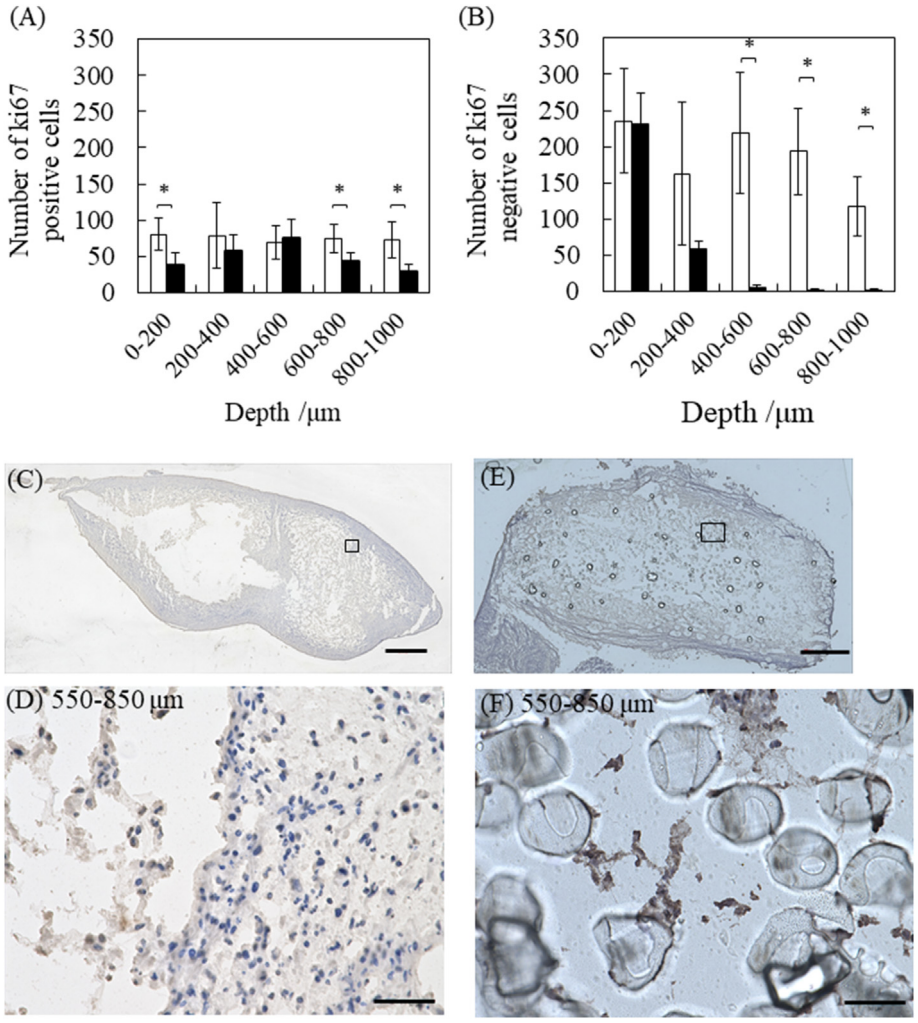

Fig. 5. Distribution of Ki67-positive and -negative cells in GHNF and PPNF 35 days after stirring culture. Depth profiles of the number of Ki67-positive (A) and -negative cells (B) in GHNF (□) and PPNF (■) 35 days after stirring culture. The cross-sectional images of GHNF (C, D) and PPNF (E, F) 35 days after stirring culture. Ki67 immunostainig images at whole of GHNF (C) and PPNF (E) and 550–850 μm depth from the surface of GHNF (D) and PPNF (F). The scale bar indicates 1 mm (C, E) and 50 μm (D, F). *, $p < 0.05$; significant difference between the two groups.

depth range of GHNF and PPNF on 35 days culture. The sGAG at 200–1200 μm depth of the GHNF was thick and bundle (Fig. 6Q, S, U, W, and Y), whereas that of PPNF was thin and spread-shaped (Fig. 6R, T, V, X, and Z). In addition, the gelatin fibers of GHNF disappeared and replaced by collagen and sGAG with an increased depth. At the 1000–1200 μm depth of GHNF, the gelatin fibers remained in the initial spherical shape although they adhered, while some cells adhered on the surface of gelatin fibers. The collagen and sGAG were present around the cells and connected between the cells and the gelatin fibers (Fig. 6E and Q). At the 600–1000 μm depth, gelatin fibers were segmented and connected by collagen and sGAG to each other. Some cells were embedded by collagen and sGAG secreted (Fig. 6G, I, S, and U). At the 200–600 μm depth, gelatin fibers almost disappeared while a network structure including collagen and sGAG was formed. Many cells were present in the collagen and sGAG network. The network structure tended to become fine and high density with a decrease in the depth (Fig. 6K, M, W, and Y). On the other hand, the PP fibers of PPNF did not disappear and few cells attached to PP fibers. Collagen and sGAG were seen separately without attached to the PP fibers (Fig. 6F, H, J, L, N, R, T, V, X, and Z).

4. Discussion

Gelatin hydrogel nonwoven fabrics (GHNF) were prepared by the simple blow spinning [24,30,32]. The diameter of gelatin fibers in GHNF is easily controlled by changing the discharge pressure in preparation and the fibers are melt-connected at the cross-point of fibers (Fig. 1C). This fiber's crosslinked intra-network structure prevent slippage between contacting fibers during deformation of nonwoven and enhanced modulus and deformation recovery property. Chavoshnejad et al. reported mechanical properties of nanofiber nonwoven enhanced according to bonded percentage of contacting fibers became higher [43]. So far, a poor mechanical property was one of the problems for gelatin usage as the cell scaffold. This formulation is one method to tackle this problem. It is difficult to maintain the pore structure of hydrogel in a wet condition during cell culture. Several methods have been reported to improve the mechanical property. There are reports on the usage of specific reagents and mixing with other materials [27–29]. Shi et al. reported that a silk-mixed gelatin scaffold improved the compressive modulus to approximately three times from the gelatin only [28]. Laronda et al. reported the chemically crosslinked gelatin 3D

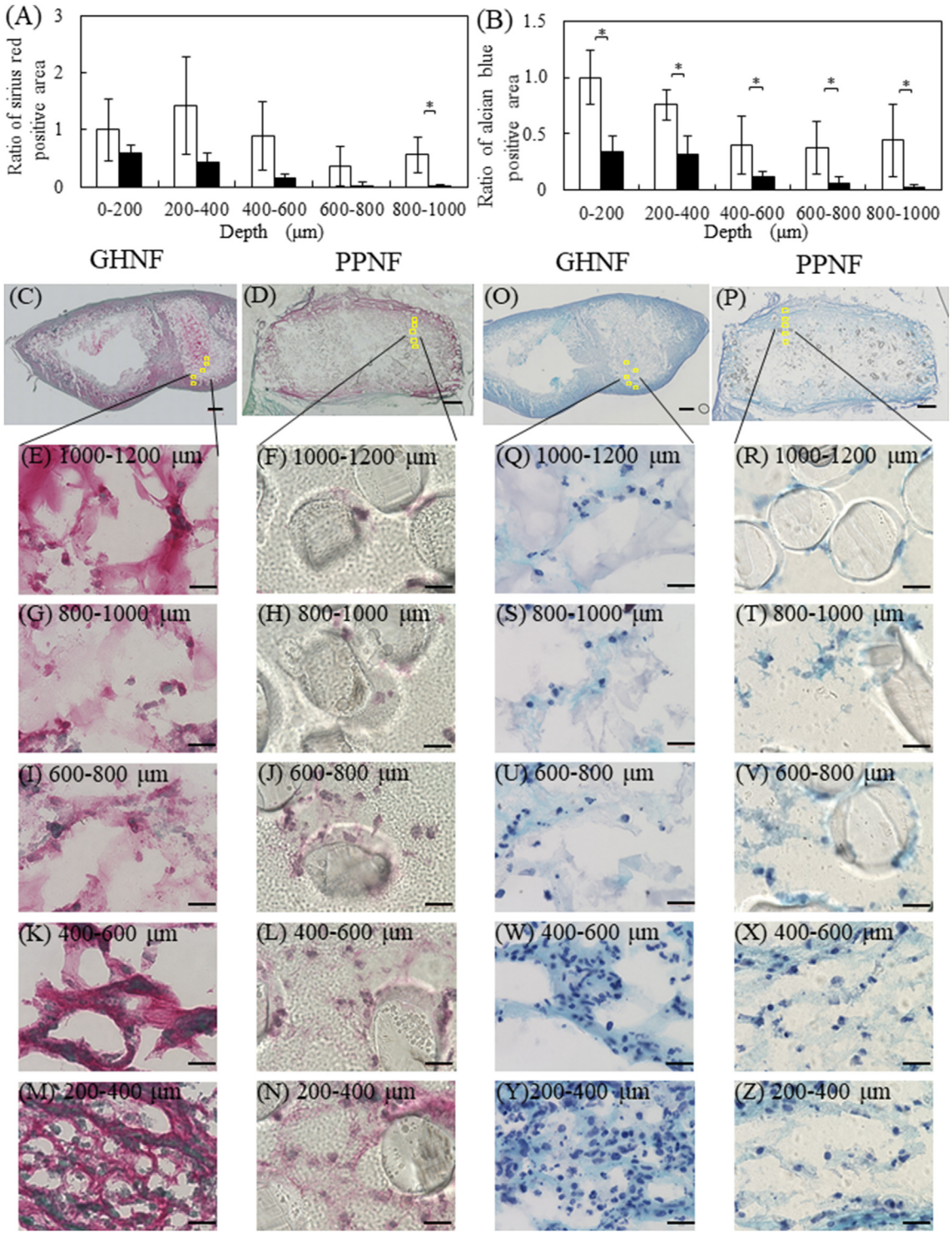

Fig. 6. Distribution of sirius red/fast green- and alcian blue-positive area in GHNF and PPNF 35 days after stirring culture. Depth profiles of sirius red- (A) and alcian blue- (B) positive area in GHNF (□) and PPNF (■) 35 days after stirring culture. Distribution of sirius red/fast green-positive area images of GHNF (C, E, G, I, K, M) and PPNF (D, F, H, J, L, N) 35 days after stirring culture at whole images (C, D) 1000–1200 (E, F), 800–1000 (G, H), 600–800 (I, J), 400–600 (K, L), and 200–400 μm (M, N) depth from the surface. Distribution of alcian blue-positive area images of GHNF (O, Q, S, U, W, Y) and PPNF (P, R, T, V, X, Z) 35 days after stirring culture at whole images (O, P), 1000–1200 (Q, R), 800–1000 (S, T), 600–800 (U, V), 400–600 (W, X), and 200–400 μm (Y, Z) depth from the surface. The scale bar indicates 500 μm (C, D, O, P) and 50 μm (E, F, G, H, I, J, K, L, M, N, Q, R, S, T, U, V, W, X, Y, Z). *, $p < 0.05$; significant difference between the two groups.

printing scaffold to increase the modulus (16.84 kPa) [29]. Liu et al. showed a high compressive modulus of a chemically crosslinked gelatin nanofibrous scaffold than the commercial gelatin sponge and the shape maintenance during the 3D culture [27]. Chang et al. prepare a hyaluronic acid mixed gelatin sponge scaffold with a compressive modulus of 22.4–43.9 kPa and a good compressive recovery property at 0–30% strain [44]. Comparing with the research results, GHNF showed both the low modulus (10 kPa) and

excellent compressive recovery property (at 70% strain) by a good contrive of a nonwoven fabrics formulation even although they are prepared from gelatin only (Fig. 1H).

To evaluate the feasibility of GHNF as a 3D scaffold, the PPNF with the similar structure was used as a control. It was apparent from the HE staining images that cells were attached onto the fiber surface both of GHNF (Fig. 2F) and PPNF (Fig. 2G), but the density of attached cells for GHNF was larger than that of PPNF. In terms of cell attachment, the GHNF was superior to PPNF as the cell scaffold. Over 14 days culture, the cell infiltration of GHNF was significantly higher than that of PPNF (Fig. 3F, H, J, P, R, and T) while the thickness of cell layers covered on the GHNF surface was significantly thinner than that of PPNF (Fig. 3E, G, Q, and S). The cells distribution analysis revealed that the number of cells at the 600–1000 μm depth in GHNF was significantly larger than that of PPNF (Fig. 4A and B). The percentage of TUNEL and HIF-1α-positive cells in GHNF at the 600–1000 μm depth was significantly smaller than that of PPNF (Fig. 4G, H, M, and N). Based on these findings, it is highly conceivable that the GHNF have a nature good enough to promote the diffusion of oxygen or the nutrient through the cell-GHNF construct, resulting in a reduced cell apoptosis. In addition, the number of Ki67-positive and -negative cells at the 600–1000 μm depth in GHNF was significantly larger than that of PPNF (Fig. 5A and B). Even if cells covered on the surface of scaffolds, it is likely that the oxygen and nutrient diffuse into the GHNF through the water phase of gelatin hydrogel fibers. As the result, the cells can be infiltrated into deeper portion for GHNF, in remarked contract with PPNF. Based on the GHNF characteristics, cells were proliferated even inside the scaffold while only the thinner cell layers were formed on the surface. Sachlos et al. suggest that cells on the top layer of scaffolds consumed most of oxygen and nutrients and the concentration of oxygen available reduces with an increase in the depth of scaffold. Eventually, the cellular migration is stopped due to the lack of oxygen and nutrients supply [14]. Such a typical behavior of cell migration was observed for the PPNF. On the contrary, due to the good oxygen and nutrients permeation through the hydrogel fibers, deeper infiltration of cells and larger number of cells proliferated even at the deep portion were achieved for the GHNF. The incorporation of gelatin hydrogel microspheres in 3D cell constructs enabled cells to enhance their survival and biological functions [20–24]. However, the utility of gelatin hydrogels as a 3D scaffold was not always clear. This study clearly demonstrates that GHNF are superior to PPNF in terms of reduced cell apoptosis and maintained the activity of cell proliferation by the improved condition of oxygen and nutrient supplies. This is experimentally confirmed by a reduced HIF-1α-positive cells number (Fig. 4M, N, and P). Moreover, the number of cells proliferated, the percentage of TUNEL- and HIF-1α-positive cells, and Ki67-positive cells at the 600–1000 μm depth in GHNF after 35 days culture, were higher than those of PPNF (Figs. 4B, H,N, and 5A) even though the gelatin fibers of GHNF disappeared (Figs. 3I, J, 4C, and D). On 7 days culture, there was significantly difference in the number of apoptotic and HIF-1α-positive cells between GHNF and PPNF (data not shown). It has been known that cells embedded in collagen and ECM gels become an apoptotic state when the gel depth became larger than 150–200 μm thickness [13]. Moreover, Colom et al. reported that the oxygen pressure was 10 mmHg in the ECM gels cultured cells for 46 h [45]. Bone marrow derived MSC became to be apoptotic when the oxygen pressure was lower than 7–24 mmHg (1–3% pO_2) [46,47]. Although the oxygen concentration in GHNF did not measure directly, we can say with certainty that oxygen condition in the GHNF was satisfied to maintain the survival and biological functions of cells.

HE staining images at different culture days revealed that the gelatin fibers were deformed and degraded around the scaffold surface where many cells were present (Fig. 3). It is known that the *in vivo* degradation of gelatin is derived by MMP-2 and -9 produced from cells [48]. The amount of MMP-2 and -9 produced may change by altering the number of cells. The cell number tended to become higher around the surface of GHNF scaffold. It is apparent that oxygen and nutrient conditions in GHNF are superior to those of PPNF (Fig. 4M and N). However, it is possible that the oxygen and nutrients are gradually consumed with an increase depth in GHNF by cells, resulting in generation of the gradient concentration of oxygen. This is one of the reasons that the number of cells proliferated and the percentage of HIF-1α-positive cells show the depth dependence of GHNF.

Sirius red staining and alcian blue staining analysis of cells in GHNF and PPNF of 35 days culture indicate that both the collagen and sGAG of representation ECM components were well secreted at the site close to the scaffold surface. The amount of collagen and sGAG for the GHNF was larger and thicker than that of PPNF (Fig. 6). The results can be also explained in terms of the superior oxygen and nutrient conditions of GHNF. It is likely that the superior conditions enable cells to proliferate and function well, resulting in an enhanced ECM secretion even in the deep portion of scaffold. In addition, the gelatin itself has an affinity for the ECM component via secreted protein like fibronectin [25,49,50]. Consequently, the collagen and sGAG would be biologically bound on the surface of gelatin fibers.

The gradual degradation of fibers in GHNF depending on the scaffold depth would be useful to from the viewpoint of the ECM remodeling process. Cell staining analysis at different depth of GHNF on 35 days culture may be effective to discuss the ECM remodeling behavior inside GHNF (Fig. 6C, E, G, I, K, M, O, Q, S, U, W, and Y). In the connection, it is necessary to consider the ECM remodeling by the following points. First, some cells were present on the surface of gelatin fibers, while the collagen and sGAG were well associated on gelatin fibers (Fig. 6E and Q). Second, when gelatin fibers started to degrade with an increased cell number, the gelatin fibers adhered to each other via collagen and sGAG associated on the surface of gelatin fibers, and then the network structure was formed. Embedment of several cells in collagen and sGAG secreted was observed (Fig. 6G, L, S, and U). Thirdly, the network structure became fine and high density with the further degradation of gelatin fibers and the generation of ECM, and many cells existed in the collagen and sGAG network (Fig. 6K, M, W, and Y). The inner porous structure of GHNF was maintained even by an increase of cell number and collagen and sGAG secretion. It is highly conceivable that collagen and sGAG were well associated with gelatin fibers and the consequent formation of network structure between cells and the gelatin fibers. As the results, the collagen and sGAG network structure was maintained even after degradation of gelatin fibers and the network structure would contribute to continued oxygen and nutrient supply into 3D cell constructs. In addition, the ECM network structure formed is real scaffold for cells, which enables cells to maintain or enhance their biological functions.

The biodegradable GHNF is a promising 3D scaffold which allows cells to proliferate homogeneously in the scaffold, secrete ECM efficiently and enhance their survival rate of cells with the apoptosis reduced. One of the applications is to provide a cell scaffold for construction of 3D cell aggregate for drug research and development. It is necessary to improve *in vitro* cell assay models for more precise prediction of drug candidate [51]. The 3D cell aggregate after degraded GHNF are highly organized from proliferated cells and secreted ECM. These cell–cell interaction and cell-ECM interaction are expected to mimic *in vivo* situations. In addition, future application of GHNF is a cell scaffold for to enhance the tissue regeneration. When GHNF are transplanted into the defect of

tissue to reconstruction, promotion of angiogenesis is expected because stromal cells and endothelial progenitor cells are infiltrated into GHNF via the interconnected porous structure. Consequently, the ECM production and the subsequent tissue formation are also expected to promote.

However, further studies are needed to make clear about the correlation among the oxygen supply, the cell survival and the ECM secretion through the biochemical analysis and measurements of partial oxygen pressure. In addition, to promote the cell survival rate, ECM remodeling, and angiogenesis in the GHNF for usage of tissue reconstruction scaffold, the structure and characteristic of GHNF, such as the diameter of gelatin fibers, the pore size, the density and degradation period, should be optimized.

5. Conclusion

When the GHNF were used to formulate a 3D cell construct, GHNF had a mechanical property sufficient enough not to deform the shape during cell culture. When the inner distribution of cells in GHNF, the apoptosis, HIF-1α, KI67, collagen or sGAG secretions of hMSC were evaluated, the cells were homogeneously proliferated inside the GHNF from the surface to the 1000 μm depth. The number of apoptosis and HIF-1α-positive cells was significantly low compared with that of PPNF as a control material. Moreover, the secretion of collagen and sGAG in GHNF was significantly superior to that of PPNF. The GHNF were degraded with the time of cell culture, and completely replaced by the collagen and sGAG secreted. It is concluded that the GHNF is a promising cell culture scaffold to formulate 3D cell constructs.

Declaration of competing interest

The authors declare that they have no known competing financial interests or personal relationships that could have appeared to influence the work reported in this paper.

Appendix A. Supplementary data

Supplementary data to this article can be found online at https://doi.org/10.1016/j.reth.2021.09.008.

References

[1] Pampaloni F, Reynaud EG, Stelzer EHK. The third dimension bridges the gap between cell culture and live tissue. Nat Rev Mol Cell Biol 2007;8:839–45.
[2] Griffith GL, Swartz AM. Capturing complex 3D tissue physiology in vitro. Nat Rev Mol Cell Biol 2006;7:211–24.
[3] Baharvand H, Hashemi SM, Ashtiani SK, Farrokhi A. Differentiation of human embryonic stem cells into hepatocytes in 2D and 3D culture systems in vitro. Int J Dev Biol 2006;50:645–52.
[4] Hirschhaeuser F, Menne H, Dittfeld C, West J, Mueller-Klieser W, Kunz-Schughart LA. Multicellular tumor spheroids: an underestimated tool is catching up again. J Biotechnol 2010;148:3–15.
[5] Pickl M, Ries CH. Comparison of 3D and 2D tumor models reveals enhanced HER2 activation in 3D associated with an increased response to trastuzumab. Oncogene 2009;28:461–8.
[6] Tung YC, Hsiao AY, Allen SG, Torisawa Y, Hoc M, Takayama S. High-throughput 3D spheroid culture and drug testing using a 384 hanging drop array. Analyst 2011;136:473–8.
[7] Imamura Y, Mukohara T, Shimono Y, Funakoshi Y, Chayahara N, Toyoda M, et al. Comparison of 2D- and 3D-culture models as drug-testing platforms in blest cancer. Oncol Rep 2015;33:1837–43.
[8] Memon AI, Sawa Y, Fukushima N, Matsumiya G, Miyagawa S, Taketani S, et al. Repair of impaired myocardium by means of implantation of engineered autologous myoblast sheets. J Thorac Cardiovasc Surg 2005;130:1333–41.
[9] Karageorgiou V, Kaplan D. Porosity of 3D biomaterial scaffolds and osteogenesis. Biomaterials 2005;26:5474–91.
[10] Zeltinger J, Sherwood J, Graham DA, Mueller R, Griffith LG. Effect of pore size and void fraction on cellular adhesion, proliferation, and matrix deposition. Tissue Eng 2001;7:557–72.
[11] Lovett M, Lee K, Edwards A, Kaplan DL. Vascularization strategies for tissue engineering. Tissue Eng B Rev 2009;15:353–70.
[12] Rouwkema J, Rivron NC, Blitterswijk CA. Vascularization in tissue engineering. Trends Biotechnol 2008;26:434–41.
[13] Szot CS, Buchanan CF, Freeman JW, Rylander MN. 3D in vitro bioengineered tumors based on collagen I hydrogels. Biomaterials 2011;32:7905–12.
[14] Sachlos E, Czernuszka JT. Making tissue engineering scaffolds work. Review on the application of solid freeform fabrication technology to the production of tissue engineering scaffolds. Eur Cell Mater 2003;5:29–40.
[15] Paciello A, Amalfitano G, Garziano A, Urciuolo F, Netti NA. Hemoglobin-conjugated gelatin microsphere as a smart oxygen releasing biomaterial. Adv Healthc Mater 2016;5:2655–66.
[16] Farris AL, Rindone AN, Grayson WL. Oxygen delivering biomaterials for tissue engineering. J Mater Chem B 2016;4:3422–32.
[17] Anada T, Fukuda J, Sai Y, Suzuki O. An oxygen-permeable spheroid culture system for the prevention of central hypoxia and necrosis of spheroids. Biomaterials 2012;33:8430–41.
[18] Martina Y, Vermette P. Bioreactors for tissue mass culture: design, characterization, and recent advances. Biomaterials 2005;26:7481–503.
[19] Kojima N, Takeuchi S, Sakai Y. Fabrication of microchannel networks in multicellular spheroids. Sensor Actuator B Chem 2014;198:249–54.
[20] Mihara H, Kugawa M, Sayo K, Tao FG, Shinohara M, Nishikawa M, et al. Improved oxygen supply to multicellular spheroids using a gas-permeable plate and embedded hydrogel beads. Cells 2019;8:525.
[21] Hayashi K, Tabata Y. Preparation of stem cell aggregates with gelatin microspheres to enhance biological functions. Acta Biomater 2011;7:2797–803.
[22] Tajima S, Tabata Y. Preparation and functional evaluation of cell aggregates incorporating gelatin microspheres with different degradabilities. J Tissue Eng Regen Med 2013;7:801–11.
[23] Matsuo T, Masumoto H, Tajima S, Ikuno T, Katayama S, Minakata, et al. Efficient long-term survival of cell grafts after myocardial infarction with thick viable cardiac tissue entirely from pluripotent stem cells. Sci Rep 2015;5:16842.
[24] Nakamura K, Saotome T, Shimada N, Matsuno K, Tabata Y. A gelatin hydrogel nonwoven fabric facilitates metabolic activity of multilayered cell sheets. Tissue Eng C 2019;25:344–52.
[25] Vlierberghe SV, Dubruel P, Schacht E. Biopolymer-based hydrogels as scaffolds for tissue engineering applications: a review. Biomacromolecules 2011;12:1387–408.
[26] Young S, Wong W, Tabata Y, Mikos AG. Gelatin as a delivery vehicle for the controlled release of bioactive molecules. J Contr Release 2005;109:256–74.
[27] Liu X, Smith LA, Hu J, Ma PX. Biomimetic nanofibrous gelatin/apatite composite scaffolds for bone tissue engineering. Biomaterials 2009;30:2252–8.
[28] Shi W, Sun M, Hu X, Ren B, Cheng J, Li C, et al. Structurally and functionally optimized silk-fibroin-gelatin scaffold using 3D printing to repair cartilage injury in vitro and in vivo. Adv Mater 2017;29:1701089.
[29] Laronda MM, Rutz LA, Xiao S, Whelan AK, Duncan EF, Roth WE, et al. A bioprosthetic ovary created using 3D printed microporous scaffolds restores ovarian function in sterilized mice. Nat Commun 2017;8:15261.
[30] Matsuno K, Saotome T, Shimada N, Nakamura K, Tabata Y. Effect of cell seeding methods on the distribution of cells into the gelatin hydrogel nonwoven fabric. Regen Ther 2020;14:160–4.
[31] Tamada Y, Ikada Y. Cell adhesion to plasma-treated polymer surfaces. Polymer 1993;34:2208–12.
[32] Medeiros ES, Glenn GM, Klamczynski AP, Orts WJ, Mattoso LHC. Solution blow spinning: a new method to produce micro- and nanofibers from polymer solutions. J Appl Polym Sci 2009;113:2322–30.
[33] Ozeki M, Tabata Y. In vivo degradability of hydrogels prepared from different gelatins by various cross-linking methods. J Biomater Sci Polym Ed 2005;16:549–61.
[34] He N, Ke Q, Huang C, Yang J, Guo Y. Needle-punched nonwoven matrix from regenerated collagen fiber for cartilage tissue engineering. J Appl Polym Sci 2014;131:40404.
[35] Li Y, Ma T, Yang ST, Kniss DA. Thermal compression and characterization of three-dimensional nonwoven PET matrices as tissue engineering scaffolds. Biomaterials 2001;22:609–18.
[36] Okamoto T, Aoyama T, Nakayama T, Nakamata T, Hosaka T, Nishijo K, et al. Clonal heterogeneity in differentiation potential of immortalized human mesenchymal stem cells. Biochem Biophys Res Commun 2002;295:354–61.
[37] Takahashi T, Tabata Y. Homogeneous seeding of mesenchymal stem cells into nonwoven fabric for tissue engineering. Tissue Eng 2003;9:931–8.
[38] Rao J, Otto WR. Fluorimetric DNA assay for cell growth estimation. Anal Biochem 1992;207:186–92.
[39] Yasuda K, Inoue S, Tabata Y. Influence of culture method on the proliferation and osteogenic differentiation of human adipo-stromal cells in nonwoven fabrics. Tissue Eng 2004;10:1587–96.
[40] Kawamoto T. Use of a new adhesive film for the preparation of multi-purpose fresh-frozen sections from hard tissues, whole-animals, insects and plants. Arch Histol Cytol 2003;66:123–43.
[41] Segnani C, Ippolito C, Antonioli L, Pellegrini C, Blandizzi C, Dolfi A, et al. Histochemical detection of collagen fibers by Sirius Red/Fast Green is more sensitive than van Gieson or Sirius Red alone in normal and inflamed rat Colon. PLoS One 2015;10:e0144630.

[42] Tam H, Zhang W, Feaver RK, Parchment N, Sacks SM, Vyavahara N. A novel crosslinking method for improved tear resistance and biocompatibility of tissue based biomaterials. Biomaterials 2015;66:83–91.
[43] Chavoshnejad P, Razavi MJ. Effect of the interfiber bonding on the mechanical behavior of electrospun fibrous mats. Sci Rep 2020;10:7709.
[44] Chang KM, Liao HT, Chen JP. Preparation and characterization of gelatin/hyaluronic acid cryogels for adipose tissue engineering: in vitro and in vivo studies. Acta Biomater 2013;9:9012–26.
[45] Colom A, Galgoczy R, Almendros I, Xaubet A, Farr R. Oxygen diffusion and consumption in extracellular matrix gels: implications for designing three-dimensional cultures. J Biomed Mater Res A 2014;102A:2776–84.
[46] Deschepper M, Oudina K, David B, Myrtil V, Collet C, Bensidhoum M, et al. Survival and function of mesenchymal stem cells (MSCs) depend on glucose to overcome exposure to long-term, severe and continuous hypoxia. J Cell Mol Med 2011;15:1505–14.
[47] Zhu W, Chen J, Cong X, Hu S, Che X. Hypoxia and serum deprivation-induced apoptosis in mesenchymal stem cells. Stem Cell 2006;24:416–25.
[48] Bonnans C, Chou J, Werb Z. Remodelling the extracellular matrix in development and disease. Nat Rev Mol Cell Biol 2014;15:786–801.
[49] Vlierberghe SV, Vanderleyden E, Dubruel P, Vos FD, Schacht E. Affinity study of novel gelatin cell carriers for fibronectin. Macromol Biosci 2009;9:1105–15.
[50] Engvall E, Ruoslahti E. Binding of soluble form of fibroblast surface protein, fibronectin, to collagen. Int J Cancer 1977;20:1–5.
[51] Breslin S, O'Driscoll L. Three-dimensional cell culture: the missing link in drug discovery. Drug Discov Today 2013;18:240–9.